Selenium distribution in French forests: Influence of environmental conditions

Paulina Pisarek, Maïté Bueno, Yves Thiry, Manuel Nicolas, Hervé Gallard, Isabelle Le Hécho

Title

Selenium distribution in French forests: influence of environmental conditions

Paulina Pisarek[1,2], Maïté Bueno[1], Yves Thiry[2], Manuel Nicolas[3], Hervé Gallard[4], Isabelle Le Hécho[1]

[1] CNRS/Univ. Pau & Pays de l'Adour/E2S UPPA, Institut des Sciences Analytiques et de Physico-Chimie pour l'Environnement et les Matériaux (IPREM), UMR 5254, 64053 Pau, France (*pisarek.paulina@univ-pau.fr) (maite.bueno@univ-pau.fr; isabelle.lehecho@univ-pau.fr)

[2] Andra, Research and Development Division, Parc de la Croix Blanche, 92298 Châtenay-Malabry Cedex, France (yves.thiry@andra.fr)

[3] Office National des Forêts (ONF), Direction Forts et Risques Naturels, Département Recherche, Développement, Innovation, Boulevard de Constance, 77300, Fontainebleau, France (manuel.nicolas@onf.fr)

[4] IC2MP UMR 7285, Université de Poitiers, 86073 Poitiers Cedex 9, France (herve.gallard@univ-poitiers.fr)

Highlights

- Statistical study of factors influencing Se distribution in 51 French forests
- Selenium concentration in litterfall increases with proximity to the ocean
- Low degradation rate of organic matter contribute to high Se stock in mor humus
- Aluminium, iron and organic matter content promote Se retention in soil

Abstract

Selenium is a trace element and an essential nutrient. Its long-lived radioisotope, selenium 79 is of potential radio-ecological concern in surface environment of deep geological repository for high-level radioactive waste. In this study, the influence of environmental, climatic and geochemical conditions on stable Se (as a surrogate of ^{79}Se) accumulation was statistically assessed (PCA analysis, Kruskall-Wallis and Spearman tests) based on the analysis of its concentration in litterfall, humus, and soil samples collected at 51 forest sites located in France. Selenium concentrations were in the ranges: 22-369, 57-1608 and 25-1222 µg kg^{-1} respectively in litterfall, humus, and soil. The proximity of the ocean and oceanic climate promoted Se enrichment of litterfall, likely due to a significant reaction of wet deposits with forest canopy. Se content was enhanced by humification (up to 6 times) suggesting that Se concentrations in humus were affected by atmospheric inputs. Selenium stock in humus decreased in the order of decreasing humus biomass and increasing turnover of organic matter: mor > moder > mull. Positive correlations between Se content and geochemical parameters such as organic carbon content, total Al and total Fe confirmed the important role of organic matter (OM) and mineral Fe/Al oxides in Se retention in soils.

Graphical abstract

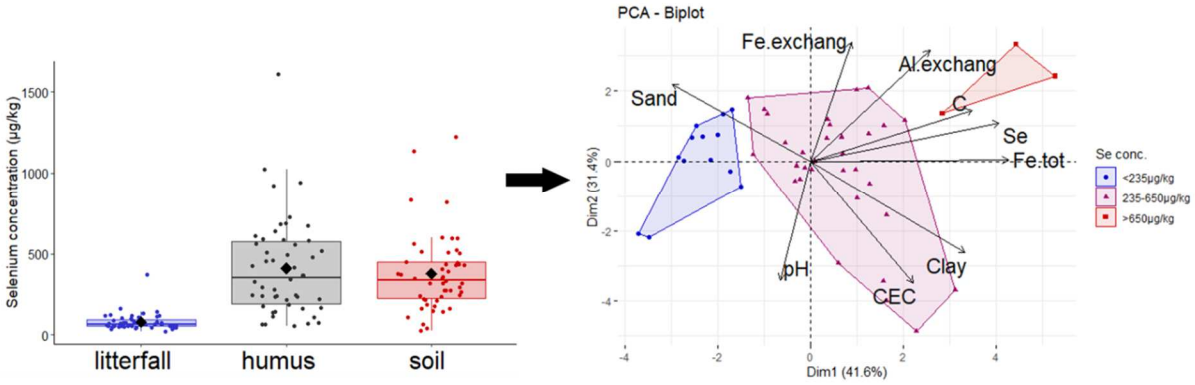

Keywords

^{79}Se, Fe exchange, pH, CEC, humification, atmospheric deposition

1. Introduction

The radionuclide ^{79}Se is of potential radio-ecological concern at high-level nuclear waste storage sites (Hjerpe and Broed, 2010) due to its long half-life (3.27×10^5 years) and its capacity to be easily incorporated into natural biogeochemical cycle. Selenium is an essential element in animal nutrition and metabolism with a major physiological role associated with its presence in amino acids as selenocysteine (SeCys) and selenomethionine (SeMet) (Rayman, 2000). Selenium is not essential for higher plants, although it is absorbed by plants to various extent with some positive effects observed, especially for hyperaccumulators (El Mehdawi and Pilon-Smits, 2012).

The global average Se content in the Earth' crust is estimated to be 50 µg kg^{-1} (Taylor and McLennan, 1995), while average Se concentration in soil is 400 µg kg^{-1} (Natasha et al., 2018). Selenium accumulation in surface soils depends on different Se inputs with variable contributions. Geogenic sources appears to be the most important for Se-rich soils only, but it does not explain the large-scale distribution of Se (Blazina et al., 2014). The ocean is an important reservoir of Se, from where it can be volatilized and transported as sea spray (Blazina et al., 2014; Sun et al., 2016; Mason et al., 2018). Therefore, atmospheric deposition to nearby coast lines influences the Se content of vegetation and soil (Låg and Steinnes, 1978), but there is little evidence of oceanic transfer to more remote terrestrial regions (Blazina et al., 2014). Thus, another contribution to soil reserves appears to originate from intermediate zones due to remobilization through volatilization, and subsequent wet and dry deposition (Ross, 1985; Suess et al., 2019). In addition to natural sources, significant anthropogenic Se contamination may come from dust, coal or petroleum combustion, as well as agricultural sludges and fertilizers (Belon et al., 2012; Natasha et al., 2018)

The mobility of Se in soil is affected by various biological and geochemical factors such as redox potential, pH, salinity, microbial activity, soil organic matter, and minerals such Fe and

Al oxides and clay (Dinh et al., 2017; Li et al. 2017). Among soil components, Fe/Al minerals and organic matter (OM) play a pivotal role in Se persistence, but there is still no agreement on the most important constituent (Coppin et al., 2009; Söderlund et al., 2016). It is also due to complex, and yet unclear, Se-OM interaction mechanisms that have been hypothesized to be mediated by mineral surfaces (Coppin et al., 2006) or by metal cations within ternary complexes (Li et al., 2017; Martin et al., 2017; Tolu et al., 2014). In soil, Se occurs in inorganic forms: Se(IV), Se(VI), Se(0), Se(-II) and in organic forms as complexes with OM or organo-mineral colloids (Winkel et al., 2015). The Se content associated with the organic fraction of soils ranges from 14 to 82% (Supriatin et al., 2015; Tolu et al., 2011; Wang et al., 2012). In forest soils around 67 ± 19% of total Se is found in the organic fraction, while it is 35 ± 12% in cultivated soils and 55 ± 22% in grasslands (Tolu et al., 2014).

Limited data are available on Se content in forest compartments (Almahayni et al., 2017; Di Tullo, 2015; Tolu, 2012; Tyler, 2005), especially in contrasted geogenic ecosystems. In this study, particular attention was paid to forest ecosystems where Se inventories are expected to characterize the long-term influence of natural inputs and element recycling processes. Here, a comprehensive statistical study was proposed to determine the significance of eco-climatic and geochemical conditions in Se accumulation and distribution at various forest sites. The concentrations of selenium were determined in litterfall, humus, and soil samples from 51 different forest sites located in France. Fluxes and stocks of Se in forest compartments were estimated, as well as time-scale involved in Se retention in humus and soil. Monitored sites showed a wide variety in types of trees, climates, soils, and distance to coast. The sample collection presented also the considerable benefit of complete characterization and regular monitoring of forest sites provided by the ONF-RENECOFOR network (National Network for the long term Monitoring of Forest Ecosystems).

2. Material and methods

2.1. Study sites

Samples of soil, humus, and litterfall were obtained from the RENECOFOR network handled by ONF (French National Forest Office), which is part of the Pan-European ICP Forests intensive (Level II) monitoring network. In order to benefit from available samples and data, the same samples from 51 sites used by Redon et al. (2011) and Roulier et al. (2019) were analyzed (Figure SI-1). These sites represent various forest types (dominance of 8 tree species), climates (continental, transition, oceanic and mountainous), humus forms (mor, moder, mull) and pedological properties (Table SI-1). The extensive data collection and sites description was carried out as part of the RENECOFOR network (Brêthes , Urlich , 1997; Probst et al., 2003; Redon et al., 2011; Roulier et al., 2019) (Table SI-2). Moreover Se concentrations and fluxes in rainfall were measured by Roulier et al., (2020) in a subset of 27 sites. The maps with the location of the sampling sites was adapted in R Studio (R Core Team, 2013; version 3.4.3). The coastal distance was estimated taking into account the closest coast and the direction of the prevailing wind.

2.2 Sampling procedure and sample treatment

Mineral soil layers of systematic depth (0-10, 10-20, 20-40 cm) and humus horizons (litter, fragmented, and humic layers) were sampled during the period 1993-1995 to measure their dry mass and chemical concentrations. For each site and layer, five samples were taken for chemical analyses from five 13.5 ×13.5 m^2 subplots distributed within the 0.5 ha central part of the site, then oven-dried at 35°C and stored in the dark at room temperature (details in Jonard et al., 2017). Litterfall was collected in ten traps of 0.5 m^2 placed at 1 m above forest floor in every plots. Litterfall samples were harvested three to five times a year in the period 1998-1999, dried and homogenized. Soil, humus and litterfall composites were prepared by mixing and grinding the individual samples in their respective mass proportions: soil layers

(0-10, 10-20, 20-40 cm), humus fractions (litter, fragmented and humic layers), and litterfall (foliage, branches, fruits and 'rest material').

2.3 Selenium extractions and analysis

Approximately 0.25 g of soil, humus, or plant material were weighed in 50 ml DigiTUBE (polypropylene). Soil was mixed with 0.5 mL of HCl and 1.5 mL of HNO_3, while humus and litterfall were mixed with 2 mL of HNO_3, 0.5 mL of H_2O_2 and 3 mL of ultrapure water (18.2 MΩ.cm, Millipore Elix system). Samples were digested at 90 °C for 3 hours in hot block digestion system (DigiPREP MS, SCP Science). Digested samples were diluted to 50 mL with ultrapure water, filtered on 0.45 µm acetate membrane and stored at 4 °C until analysis. Each sample was extracted and analyzed in triplicate except those in limited amount (detailed in Table SI-3) and blanks were added in each digestion run.

Selenium concentration was determined by inductively coupled plasma mass spectrometry (ICP-MS; 7500ce and 7900, Agilent Technologies, Tokyo, Japan) with collision/reaction cell gas flow of 5 mL min^{-1} H_2. Quantification was obtained by external calibrations in reconstituted matrices (blanks). Instrumental detection limits for Se ranged between 0.4 - 8 µg kg^{-1} depending on sample matrix. Typical analytical precision was lower than 10 % (relative standard deviation, 15 replicates). Certified reference materials of soil DC 73030, DC 73032 (National Analysis Center for Iron & Steel, Beijing, China) and vegetal material ERM-CD281 (Rye grass, Community Bureau of Reference, Brussels, Belgium) were analyzed in order to validate the accuracy of the extraction and analytical methods. Our experimental values (191 ± 15 µg kg^{-1} for DC 73030, 118 ± 9 µg kg^{-1} for DC 73032, 24 ± 3 µg kg^{-1} for ERM-CD281) agreed well with the certified values (200 ± 30 µg kg^{-1} for DC 73030, 140 ± 20 µg kg^{-1} for DC 73032, 23 ± 4 µg kg^{-1} for ERM-CD281).

2.4. Calculations

Total soil mass (g ha^{-1}) was estimated as the sum of the masses of all soil layers (0-10, 10-20, 20-40 cm) that were calculated by multiplying the soil layer density by the layer thickness. Selenium stock in the top 40 cm of soil (g ha^{-1}) was calculated by multiplying Se concentration by soil mass. Selenium stocks in humus (g ha^{-1}) and annual litterfall (g ha^{-1} yr^{-1}) were calculated by multiplying selenium concentration by the masses of corresponding compartments. Information about soil bulk densities and masses of compartments were provided by ONF and are given in Table SI-2.

Theoretical average residence time in forest soil (t_{resSe}) was calculated according to the Equation 1:

$$\mathbf{t_{resSe}} = \frac{\text{stock of Se in humus+mineral soil}}{\text{Annual wet atmospheric Se input}} \text{ (years)} \qquad (1)$$

This calculation was based on steady-state assumption and on the fact that Se input from weathering of the parent rock is negligible given the low average Se content of the Earth' crust (Taylor and McLennan, 1995). Therefore, atmospheric deposition was considered the only source of Se in the forest soil as proposed previously by Redon et al. (2011) and Bowley (2013) for chlorine and iodine. Values of annual wet atmospheric Se used for calculation were from Roulier et al. (2020).

Net Se accumulation rate in humus allowed estimating accumulation associated to vegetal material decay (from litterfall to humus) and was calculated according to Equation 2 (Redon et al., 2011):

$$\textbf{Se accumulation rate} = \frac{([\mathbf{Se}]_{\mathbf{humus}} - [\mathbf{Se}]_{\mathbf{litter}}) \times \mathbf{DM_{humus}}}{\mathbf{t_{resDM}}} \text{ (g } ha^{-1} \text{ } yr^{-1}) \qquad (2)$$

where $[Se]_{humus}$ and $[Se]_{litter}$ are Se concentrations in humus and litterfall, DM_{humus} and t_{resDM} are dry mass and the average dry matter residence time in the humus, respectively. t_{resDM} was calculated according to Equation 3 (Redon et al., 2011):

$$\mathbf{t_{resDM}} = \frac{\mathbf{DM_{humus}}}{\mathbf{LF \times (1 - litter\ fraction\ mineralized)}} \text{ (years)} \qquad (3)$$

where LF is the annual litterfall dry mass. 'litter fraction mineralized' is the average mass loss of litter due to mineralization before its total humification. For the calculation, litter fraction mineralized values were taken from the study of Osono and Takeda (2005) on different tree species (85% in pines, 70% in Douglas, 61% in spruce, 51% in silver fir, 65% in beech and 43% in oak forests).

2.5. Statistical analyses

Statistical analyses were used to determine correlations between selenium concentrations or stocks in soil, humus, and litterfall (response variables) with environmental, climatic, and geochemical conditions.

Shapiro-Wilk test was first used to determine if selenium concentrations and stocks in soil, humus and litterfall were normally distributed. As Se data were not normally distributed, a Spearman rank correlation test and Kruskal-Wallis test were performed respectively for numerical and categorical variables. Categorical variables comprised: forest type (coniferous, deciduous), tree species (oak, beech, Douglas, pine, spruce, fir), climate (mountain, continental, oceanic, transition), humus type (mor, mull, moder), rock type (sedimentary rocks, igneous rocks, other), soil type (cambisol, planosol, podzoluvisol, luvisol, andosol, podzol, letosol). Pairwise Wilcoxon test with Holm adjustment for p-values was applied in order to establish the differences within sub-groups of categorical variables.

The distributions of selenium concentrations, stocks, and accumulation rates were represented by boxplots for disparate categorical variables, with significant differences indicated by

192 letters. Principal component analysis (PCA) was performed and a biplot correlation circle
193 was drawn in order to visualise the relationships between soil numerical physico-chemical
194 parameters and selenium concentrations in soil and the contribution of individual sites into
195 the representation. Statistical analyses and boxplot representations were performed with R
196 Studio (R Core Team, 2013; version 3.4.3).
197

198 ## 3. Results and discussion

199 ### 3.1 Selenium distribution in forest ecosystems

200 Selenium concentrations in litterfall, humus, and soil samples of the forest sites are detailed
201 in Table SI-3. Selenium concentrations were in the ranges 22-369 µg kg^{-1}, 57-1608 µg kg^{-1}
202 and 25-1222 µg kg^{-1} respectively for litterfall, humus and soil samples (Figure 1).
203 Selenium concentrations in humus were in the same range or higher than in soils while in
204 litterfall they were on average 6 times lower than in humus and soils (Kruskal-Wallis rank for
205 global test: $\chi^2 = 75.30$, p-value < 0.001). Selenium contents in litterfall were comparable to
206 values of 59 ± 11 (Di Tullo, 2015) and 112 µg kg^{-1} (Tyler, 2005) previously reported for
207 beech leaf litter. A wide range of Se concentration in humus was also observed in the
208 literature. Di Tullo (2015) reported 151 µg kg^{-1} for beech mull type humus and Tyler (2005)
209 the value of 650 µg kg^{-1} for mor – humus formation of soil's O-horizon. Reimann et al.
210 (2015) also observed higher Se concentrations in the range 400-6300 µg kg^{-1} in organic O-
211 horizon compared to 100-2700 µg kg^{-1} in mineral C-horizon (20-80 cm depth) of Norwegian
212 forests. Selenium concentrations in soils (Figure 2) were coherent with average global values
213 from 10 to 2000 µg kg^{-1} (Natasha et al., 2018) and values reported for European soils: 82 to
214 1119 µg kg^{-1} in France (Tolu, 2012), 100 to 4000 µg kg^{-1} in UK (Broadley et al., 2006) and
215 120 to 1970 µg kg^{-1} in the Netherlands (Supriatin et al., 2015). Selenium concentrations in

humus were only moderately correlated with Se concentrations in litterfall (Spearman test, r_s = 0.40, $p < 0.01$), whereas no correlation was found between Se concentrations in litterfall and soil (p-value > 0.05). Moderate correlation between Se concentrations in humus and soil was found (Spearman test, $r_s = 0.43$, p-value < 0.01).

The Se stock in 40 cm deep soil composites varied from 142 to 3702 g ha^{-1}, which is much higher than Se reserves in humus (0.3 to 121 g ha^{-1}, Table SI-3). The mean annual Se flux from litterfall to forest soil was 0.30 g ha^{-1} yr^{-1} with values ranging from 0.06 to 1.20 g ha^{-1} yr^{-1} (Table SI-3). Roulier et al (2020) reported annual Se fluxes in rainfall for a subset of the same surveyed sites (n = 27) ranging from 0.25 to 2.01 g ha^{-1} yr^{-1} with a median value of 0.34 g ha^{-1} yr^{-1}. Combining these two fluxes would result into apparent total annual Se contribution to forest floor of 0.45 – 2.49 g ha^{-1} yr^{-1} (Table SI-3). The sum of these two contributions might overestimate Se input to the soil given the interception (mean annual interception fraction of the precipitation can reach 31% (Ulrich et al., 2002)) and potential surface adsorption of a fraction of Se from rain by foliage before senescence. In addition to wet deposition interception, it is also possible that Se in litterfall partly originated from dry deposition or foliar or root uptake, different pathways not considered in the present budget. On the other hand, Se volatilization that is common for many plants and microorganisms (Chasteen and Bentley, 2003) might have compensated the impact of those different processes in overall budget. In brief, the net accumulation of atmospheric Se by the foliage remains uncertain and difficult to quantify as is the case for various trace elements. Moreover, the results of correlation tests showed no direct dependence between Se concentrations in humus and soil and the sum of Se contributions from rain and litterfall ($p > 0.05$, Table 1). This suggests that mobilization and immobilization processes of Se in forest soils have a greater influence on the Se concentration of soils than the contributions of rainfall and litterfall. When Se reaches the ground via litterfall, it can be released during

biomass decomposition, then volatilized, or leached to deeper forest soil layers where sorption/desorption processes take place, or possibly taken up by tree roots and further recycled. Further statistical analyses were performed in order to highlight the factors affecting Se inventories in forest ecosystem.

3.2 Environmental factors affecting Se concentration in litterfall

Statistical analysis showed significant effect of distance from the coast, climate type, Se concentration, and flux in rain on Se concentration in litterfall (Table 1). Furthermore, Se concentration in litterfall was statistically homogeneous through forest types and tree species (Kruskal-Wallis test, $p > 0.05$).

Slightly higher concentrations of Se in litterfall in oceanic climate compared to transition and mountain climates (Figure 3.1) were confirmed by weak negative correlation between Se concentration in litterfall and distance from the coast (Spearman test, $r_s = -0.35$, $p < 0.05$). The ocean is an important source of atmospheric Se (Amouroux et al., 2001; Mason et al., 2018; Wen and Carignan, 2007), reaching the ground or plant surface as dry and wet depositions. Strong positive correlation was obtained between Se concentration in litterfall and in rainfall when EPC08 site was excluded (Spearman test, $r_s = 0.73$, $p < 0.001$, $r^2 = 0.66$, Figure 3.2). This site showed a very high Se concentration in litterfall (369 µg kg^{-1}) compared to concentrations of the other sites (between 22 and 161 µg kg^{-1}), suggesting local contamination. The high concentrations of Se in soil (1222 µg kg^{-1}) and humus (1608 µg kg^{-1}) at this site would be coherent with recurrent atmospheric emissions. The EPC08 site is located in the Ardennes mountains, very close to the industrial regions of Western Europe (Cumbers et al., 2006) whose economy had been based for years on metallurgical industry requiring charcoal combustion. Nowadays, there are developed railway, car and battery recycling industries, all of which can be a potential source of long-term local pollution.

Interestingly, the same site was also reported to be contaminated by As and atmospheric deposits of Pb (Pauget et al., 2013; Probst et al., 2003).

In summary, Se concentration in litterfall was dependent from environmental conditions such as climate, Se input from rainfall and proximity to the coast. Furthermore, anthropogenic sources may contribute to Se deposition for some sites.

3.3 Se accumulation in humus compartment

As already discussed in Section 3.1, Se concentration in humus showed a wide range of values from 57 to 1607 µg kg^{-1} with median value of 353 µg kg^{-1} and maximum value corresponding to EPC08 potentially contaminated site. According to differences between litterfall and humus, Se concentration was increased on average six times along the litter decay continuum. Generally, Se concentrations in humus of coniferous forests were higher than in deciduous forests (Figure 4.1, Table 1), despite homogenous concentrations of selenium in litterfall of both forest types. Thus, humus under spruce and Douglas had significantly higher Se content compared to oak (Figure SI-2, Table 1). It may result from differences in the humification process, as deciduous leaves have a different composition from conifer needles (e.g. lower lignin content), which generally leads to a higher labile mass content and greater leaching losses in the early stages of litter decomposition (Prescott et al., 2000). The calculated average residence times of humus where higher for Douglas fir, spruce and pine (37.6 ± 27.7, 54.2 ± 50.4 and 144.2 ± 113.5 years, Table SI-2) compared to oak and beech (5.5 ± 5.0 and 12.4 ± 12.2 years Table SI-2), which reflects slower decomposition rates of organic matter under conifers. Only humus from silver fir differed from the other coniferous species by low masses (20.3 ± 15.5 t ha^{-1}) and low average residence times (10.8 ± 6.8 years). In the RENECOFOR network, forests of silver fir were usually associated to mull humus formation on cambisol characterized by rapid litter decomposition.

As a consequence of different litter decay rates, Se concentration in humus was strongly correlated with humus mass (Spearman rank test, r_s =0.68, p-value < 0.001). This resulted in lower humus Se stocks in oak, beech and silver fir forests (4 ± 6, 8 ± 15, 10 ± 9 g ha^{-1}) compared to Douglas fir, spruce and pine (16 ± 11, 47 ± 38, 41 ± 38 g ha^{-1}). It was reflected likewise in the dependence of the Se humus stock on the type of humus. Mean Se stock in humus decreased in the order: mor > moder > mull according to decreasing humus biomass and increasing organic matter degradation rate (Figure 4.2, Table 1). Selenium concentrations in soils followed opposite order with significantly lower concentrations in soils under mor compared to mull-humus formations (Figure 4.3) highlighting the importance of Se input from humus decomposition to the underlying soil layers. Selenium can be mobilized in the form of soluble (hydr)-oxyanions and/or organo-Se compounds (seleno-methionine (SeMet) and methane seleninic acid (MeSeOOH) (Tolu et al., 2014)) and colloidal OM of plant or microbial origin (Weng et al., 2011). Beside lower biomass and faster degradation, mull-humus formation is also characterized by higher microbial activity, which can lead to the release of volatile compounds such as H_2Se, DMSe (dimethyl selenide) and DMDSe (dimethyl diselenide) into the atmosphere (Wessjohann et al., 2007).

The median Se accumulation rate in humus was 0.30 g ha^{-1} yr^{-1} with no clear distinction between coniferous and deciduous tree species (Table SI-3). The highest accumulation rate, 1.57 g ha^{-1} yr^{-1}, was for the EPC08 site. For this site, a long lasting dry deposition from anthropogenic contamination may affect accumulation rate value. Generally, Se accumulation rates were positive, except for one beech forest site (HET55: -0.02 ± 0.01 g ha^{-1} yr^{-1}) for which Se concentrations in humus and litterfall were similar (57 ± 6 and 73 ± 8, respectively, Table SI-3). Negative accumulation rates were reported for chlorine in beech and oak forests, while they were positive for chlorine in Douglas, fir, spruce, and pine forests (Redon et al., 2011), and for iodine in all tree species (Roulier et al., 2019). Negative accumulation rates

were interpreted as a result of high humus decomposition rate and leaching, whereas positive accumulation rates reflect Se enrichment during the process of litterfall transformation into humus. The average rate of Se accumulation in humus (0.39 g ha^{-1} yr^{-1}) was similar to the average Se flux from litterfall (0.30 g ha^{-1} yr^{-1}), and the average rainfall Se flux (0.44 g ha^{-1} yr^{-1}). This suggests a partial humus enrichment by the capture of soluble Se from rain through sorptive accumulation. Beside the retention, Se of atmospheric origin is subject to losses by drainage and volatilization, but the contribution of each pathway remains unclear and needs further investigation.

To conclude, Se inventories in humus were mostly controlled by the litter decay process and the rate of organic matter decomposition and not directly by the input of Se to the forest floor.

3.4 Environmental variables influencing Se content in soil

The soil compartment was shown to be the main reservoir of Se. Tree species, climate and rock type were the most discriminating categorical variables (Paragraph 3.3) to explain the variation in Se content in French forest soils. Although the ocean is an important reservoir of Se on a global scale, no direct correlation was found between Se concentration in soil and distance from the coast. Decreasing Se content was observed with the distance from the ocean in forest soil in Norway (Låg and Steinnes, 1978). Blazina et al. (2014) showed that over the last 6.8 million years the monsoonal climate had likely dominant role on atmospheric Se deposition and soil concentration in Chinese Loess Plateau. Winkel et al. (2015) highlighted the need for further research to determine the extent to which wet deposition influences soil Se levels on a large scale, although Se generally measured in wet deposition is not location-dependent. In our study higher Se concentrations in soil were only observed for the mountain climate compared to continental climate (Figure 5.1, Table 2). It may be due to reduced microbial activity and lower degradation rate of OM in colder climate

or specific soil composition in the mountain climate. The former would have minor impact, as no dependence was observed between Se concentrations in humus and climate. The latter would be more important as mountainous soils had elevated total Fe, total Al and organic C contents (Figures SI 5-7). Another co-correlation was found between climate and tree species, as Se-poor transition forest soils were dominated by pines and oaks, while Se-rich mountainous forest soils by Douglas. Summing up, the co-correlations between Fe, Al, C contents in soil, climate and tree species do not permit to determine which of these factors plays a dominant role in Se immobilization in soil.

No dependence was observed between Se concentrations in soil and soil type ($p > 0.05$, Table 2), which may be due to large variability in soil composition within a soil type. Concerning the effect of bedrock material, soils derived from sedimentary rocks were in general poorer in Se than those from igneous rocks (Figure 5.2, Table 1), which is contrary to some statements in the literature (Sharma et al., 2015). Average Se level in igneous rocks was reported as 0.35 mg kg^{-1}, while the content in sedimentary rocks varies significantly within classification groups: 0.05 mg kg^{-1} in sandstone, 0.08 mg kg^{-1} in limestone and the highest values for rocks with high organic carbon content: 0.6 mg kg^{-1} for shale and 300 mg kg^{-1} for coal (Natasha et al., 2018). Thus, Se concentrations measured in 0-40 cm soil depth may not reflect the character of rock, especially for low-Se parent materials. Additionally, as analyzed soils were from shallow soil layer (≤ 40 cm), Se input from litterfall and atmospheric depositions masks the influence of soil parent material weathering.

3.5 Effect of soil composition on Se content

A correlation matrix was first constructed with all numerical variables describing soil composition (Table SI-4). The variables that were well correlated (Spearman rank test $r_s >$ 0.6) with soil Se concentrations were total Al, total Fe, total N, organic C, and clay fraction.

366 Moreover, there were also moderate correlations with soil exchangeable Al concentration,
367 sand and silt fractions, and cation exchange capacity (CEC). PCA analysis was then used to
368 depict the effect of soil composition on Se concentrations of individual soils. Sites EPC63
369 and EPC08 were excluded in PCA analysis because they showed peculiar characteristics, as
370 highlighted by their position with respect to linear correlations between Se concentration and
371 total Fe/Al and C_{org} (Figure SI-6, r^2 = 0.75 and r^2 = 0.62, respectively). As previously
372 discussed (Section 3.2), EPC08 was identified as a potentially contaminated site. The soil at
373 EPC63 site was the only representative of Andosol, which is rare for French geographical
374 location (about 1% in France) (Quantin, 2004).
375 The contribution of each variable to the first three principal components of PCA is presented
376 in Table 2. Further, the number of variables was reduced by removing co-correlated
377 parameters. Therefore, organic C was selected as the sole representative of soil OM
378 (elimination of total N) and total Fe as the sole representative of Fe/Al minerals (elimination
379 of total Al). Mn exchangeable was excluded as it contributed little to Dim 1 and Dim 2
380 components (Table 2) and any significant effect (p-value > 0.05) of soil exchangeable Mn on
381 Se concentration was observed. It was not surprising as selenite is more readily released to
382 liquid phase by anion-exchange mechanism from Mn oxides compared to goethite (Fe
383 oxides) (Saeki and Matsumoto, 1994).
384 The first two principal components explained 73.0% of the variation (Dim1 41.6 % and Dim2
385 31.4%). Selenium, C_{org} and Fe concentrations in soil were characterized by strongly positive
386 coordinates on the Dim 1 axis (Figure 6). Moreover, PCA eigenvalues showed positive loads
387 in the Dim1 for clay, Al exchangeable, CEC and Fe exchangeable variables. The second
388 component was well described by pH and Fe exchangeable variables that were logically anti-
389 correlated. Similar anti-correlation was observed between sand and clay fractions.

390 Soil samples were discriminated in three clusters of different Se concentrations: <235 µg
391 kg^{-1}, 235-650 µg kg^{-1}, >650 µg kg^{-1}. Located on negative Dim 1, the first cluster with the
392 lowest Se concentrations < 235 µg kg^{-1} including 13 sites was characterized by soils with
393 high contribution of sand and low C_{org} and Fe/Al content. This cluster includes mainly
394 arenosols, podzols, and planosols in oceanic and transition climates with maritime pine and
395 oak as the main tree species. In this cluster, sites PM17 and PM85 are two arenosols close to
396 the ocean (≤ 2 km) with the lowest Se concentrations (25 µg kg^{-1} and 39 µg kg^{-1},
397 respectively). Their position in the biplot is explained by their very high content of sand (99%
398 and 96% respectively), high pH values (8.7 and 8.5 respectively), and low OM content (3.85
399 and 5.55 g kg^{-1} respectively). These results confirmed the importance of OM and Al/Fe
400 content in Se retention and the fact that sand fraction is a weak Se carrier (Chi et al., 2019;
401 Coppin et al., 2006; Saeki and Matsumoto, 1994).
402 At the opposite on the biplot graph, the three soils with the highest Se concentrations (> 650
403 µg kg^{-1}; HET30, DOU71 and DOU65 sites) had positive coordinates on both dimensions
404 axes associated with Se, C_{org}, total Fe and Al exchangeable variables. These soils are acidic
405 podzols (HET30 and DOU 71) or cambisol (DOU65) in mountain climate with very high C_{org}
406 (67 – 85 g kg^{-1}), Fe (8.7 – 14.3 g kg^{-1}) and Al (7.1 – 12.0 g kg^{-1}) contents. In our study the
407 concentrations of organic C (and total N) were strongly correlated with those of total Fe and
408 Al (Table SI-6). Strong correlation between Se content and organic C concentration in soil is
409 related to the ability of OM to interact with Se. Aluminium and Fe oxides remain protonated
410 in a broad pH range and have relatively large surface area with densely arrayed functional
411 groups. These functional groups can also promote the formation of inner and outer sphere
412 complexes with Se (Peak, 2006; Söderlund et al., 2016). Like in our study, hot spots of Se in
413 soils were identified as co-located with Fe and Al contents suggesting possible indirect
414 sorption on metals associated within OM surface or matrix (Coppin et al., 2009).

Soils with medium Se concentrations (235 - 650 µg kg^{-1}) were gathered in the third cluster (32 sites for a total of 49). This cluster contains all types of soils (except the two arenosols discussed previously), tree species and climates. Within this cluster, a sub-group of 4 sites (SP25, SP11, SP05 and HET25) for three soil types (luvisol, cambisol and leptosol) was characterized by a strong contribution of clay fraction (35 – 50 %) and neutral pH (5.76 – 7.21). With moderate C_{org} (23 – 31g kg^{-1}) and Al/Fe content (from 1.9 to 5.1 g Al kg^{-1} and 4.2 to 9.7 g Fe kg^{-1}), they also exhibited moderately high Se concentrations (371 – 500 µg kg^{-1}).

Summarizing all of the above, our results confirm the strong relationships between Se and organic matter and Al/Fe constituents. However, it was not possible to clarify whether Fe/Al oxides or OM have a greater influence on Se sorption, as these variables were highly correlated and may act synergistically on Se retention.

The calculated selenium residence times in forest soils (t_{resSe}) were between 617 and 8406 years (median value 2735 years for n = 27 sites), which is higher than retention times of iodine (419 - 1756 years) and chlorine (3 - 67 years) for the same sites (Redon et al., 2011; Roulier et al., 2019). That pattern is in agreement with other results showing higher desorption distribution coefficients K_D in woodland for Se (41 - 1198 L kg^{-1} (Almahayni et al., 2017; Tolu et al., 2014)) compared to I (4 - 281 L kg^{-1}) as well as higher sorption coefficient K_D values for Se (4 - 2100 L kg^{-1}) than for I (0.01 - 580 L kg^{-1}) and Cl (0.04 - 1.2 L kg^{-1}) in all types of soils (IAEA, 2010). Summing up, radionuclide ^{79}Se has a highest potential to persist in soil compartment compared to the other radionuclides ^{129}I and ^{36}Cl. The broad range of t_{resSe} is a result of combinations of local environmental factors including input to soil, organic matter turnover, and soil properties.

4. Conclusions

In this study, the influence of environmental and geochemical conditions on Se accumulation in forest soil was analyzed. Selenium concentration in litterfall was linearly dependent on its concentration in rainfall with higher values near the coast, i.e. for oceanic climate. Deviation from correlation was observed for one site with very high concentration in litterfall (369 µg/kg) and was attributed to anthropogenic activities. The annual amount of selenium cycling through litterfall was minor compared to Se stock in forest soils and, no direct correlation was found between the two. The higher Se concentrations of recalcitrant mor humus compared to easily degradable mull humus highlighted that organic matter degradation rate likely controls Se content in humus and more generally in soils. In forest soils, the content of organic matter and Fe/Al oxides had pivotal role among all soil constituents in long-term Se retention. Thus, acidic soils rich in organic matter and Fe/Al oxides under Douglas fir and beech forests in mountain climate are the soil properties and environmental conditions that promote the persistence of Se in forest soils.

Supplementary information

Additional information as noted in the text.

Acknowledgements

The authors would like to thank all technical support from the RENECOFOR-ONF network, which provided the collection of samples and sites data. We wish to acknowledge M. Roulier for her guidance with statistical program.

Funding: This research was financially supported by the French National Radioactive Waste Management Agency (Andra).

References

Almahayni, T., Bailey, E., Crout, N.M.J., Shaw, G., 2017. Effects of incubation time and filtration method on Kd of indigenous selenium and iodine in temperate soils. J. Environ. Radioact. 177, 84–90. https://doi.org/10.1016/j.jenvrad.2017.06.004

Amouroux, D., Liss, P.S., Tessier, E., Hamren-Larsson, M., Donard, O.F.X., 2001. Role of oceans as biogenic sources of selenium. Earth Planet. Sci. Lett. 189, 277–283. https://doi.org/10.1016/S0012-821X(01)00370-3

Belon, E., Boisson, M., Deportes, I.Z., Eglin, T.K., Feix, I., Bispo, A.O., Galsomies, L., Leblond, S., Guellier, C.R., 2012. An inventory of trace elements inputs to French agricultural soils. Sci. Total Environ. 439, 87–95. https://doi.org/10.1016/j.scitotenv.2012.09.011

Blazina, T., Sun, Y., Voegelin, A., Lenz, M., Berg, M., Winkel, L.H.E., 2014. Terrestrial selenium distribution in China is potentially linked to monsoonal climate. Nat. Commun. 5, 1–7. https://doi.org/10.1038/ncomms5717

Bowley, H.E., 2013. Iodine dynamics in the terrestrial environment PhD Thesis. University of Nottingham.

Brêthes A., Urlich E., 1997. Caractéristiques pédologiques des 102 peuplement du réseau. - Office national de forêts, Dépt des recherches Techniques.

Broadley, M.R., White, P.J., Bryson, R.J., Meacham, M.C., Bowen, H.C., Johnson, S.E., Hawkesford, M.J., McGrath, S.P., Zhao, F.-J., Breward, N., Harriman, M., Tucker, M., 2006. Biofortification of UK food crops with selenium. Proc. Nutr. Soc. 65, 169–181. https://doi.org/10.1079/pns2006490

Chasteen, T.G., Bentley, R., 2003. Biomethylation of selenium and tellurium: microorganisms and plants. Chem. Rev. 103, 1–25. https://doi.org/10.1021/cr010210+

Chi, F.Q., Kuang, E.J., Zhang, J.M., Su, Q.R., Chen, X.L., Zhang, Y.W., Liu, Y.D., Kuang, E.J., Zhang, J.M., Su, Q.R., Chen, X.L., Zhang, Y.W., Liu, Y.D., 2019. Fractionation and distribution of soil selenium and effects of soil properties in Heilongjiang. Selenium Research for Environment and Human Health: Perspectives, Technologies and Advancements. https://doi.org/10.1201/9780429423482-9

Coppin, F., Chabroullet, C., Martin-Garin, A., 2009. Selenite interactions with some particulate organic and mineral fractions isolated from a natural grassland soil. Eur. J. Soil Sci. 60, 369–376. https://doi.org/10.1111/j.1365-2389.2009.01127.x

Coppin, F., Chabroullet, C., Martin-Garin, A., Balesdent, J., Gaudet, J.P., 2006. Methodological approach to assess the effect of soil ageing on selenium behaviour: first results concerning mobility and solid fractionation of selenium. Biol. Fertil. Soils 42, 379–386. https://doi.org/10.1007/s00374-006-0080-y

Cumbers, A., Birch, K., MacKinnon, D., 2006. Revisiting the Old Industrial Region: Adaptation and Adjustment in an Integrating Europe. CPPR Working Paper 1. University of Glasgow.

Di Tullo, P., 2015. Dynamique du cycle biogéochimique du sélénium en écosystèmes terrestres : rétention et réactivité dans le sol, rôle de la végétation (thesis). Pau.

Dinh, Q.T., Li, Z., Tran, T.A.T., Wang, D., Liang, D., 2017b. Role of organic acids on the bioavailability of selenium in soil: A review. Chemosphere 184, 618–635. https://doi.org/10.1016/j.chemosphere.2017.06.034

El Mehdawi, A.F., Pilon-Smits, E. a. H., 2012. Ecological aspects of plant selenium hyperaccumulation. Plant. Biol. 14, 1–10. https://doi.org/10.1111/j.1438-8677.2011.00535.x

Hjerpe, T., Broed, R., 2010. Radionuclide transport and dose assessment modelling in biosphere assessment 2009 (No. POSIVA-WR--10-79). Posiva Oy.

IAEA, 2010. Handbook of Parameter Values for the Prediction of Radionuclide Transfer in Terrestrial and Freshwater Environment.

Jonard, M., Nicolas, M., Coomes, D.A., Caignet, I., Saenger, A., Ponette, Q., 2017. Forest soils in France are sequestering substantial amounts of carbon. Sci. Total Environ. 574, 616–628. https://doi.org/10.1016/j.scitotenv.2016.09.028

Låg, J., Steinnes, E., 1978. Regional distribution of selenium and arsenic in humus layers of Norwegian forest soils. Geoderma 20, 3–14. https://doi.org/10.1016/0016-7061(78)90045-9

Li, Z., Liang, D., Peng, Q., Cui, Z., Huang, J., Lin, Z., 2017. Interaction between selenium and soil organic matter and its impact on soil selenium bioavailability: A review. Geoderma 295, 69–79. https://doi.org/10.1016/j.geoderma.2017.02.019

Martin, D.P., Seiter, J.M., Lafferty, B.J., Bednar, A.J., 2017. Exploring the ability of cations to facilitate binding between inorganic oxyanions and humic acid. Chemosphere 166, 192–196. https://doi.org/10.1016/j.chemosphere.2016.09.084

Mason, R.P., Soerensen, A.L., DiMento, B.P., Balcom, P.H., 2018. The global marine selenium cycle: insights from measurements and modeling. Global Biogeochemical Cycles 32, 1720–1737. https://doi.org/10.1029/2018GB006029

Natasha, N., Shahid, M., Niazi, N.K., Khalid, S., Murtaza, B., Bibi, I., Rashid, M.I., 2018. A critical review of selenium biogeochemical behavior in soil-plant system with an inference to human health. Environ. Pollut. 234, 915–934. https://doi.org/10.1016/j.envpol.2017.12.019

Osono, T., Takeda, H., 2005. Limit values for decomposition and convergence process of lignocellulose fraction in decomposing leaf litter of 14 tree species in a cool temperate forest. Ecol. Res. 20, 51–58. https://doi.org/10.1007/s11284-004-0011-z

Pauget, B., Gimbert, F., Coeurdassier, M., Crini, N., Pérès, G., Faure, O., Douay, F., Hitmi, A., Beguiristain, T., Alaphilippe, A., Guernion, M., Houot, S., Legras, M., Vian, J.-F., Hedde, M., Bispo, A., Grand, C., de Vaufleury, A., 2013. Ranking field site management priorities according to their metal transfer to snails. Ecol. Indic. 29, 445–454. https://doi.org/10.1016/j.ecolind.2013.01.012

Peak, D., 2006. Adsorption mechanisms of selenium oxyanions at the aluminum oxide/water interface. J. Colloid Interface Sci. 303, 337–345. https://doi.org/10.1016/j.jcis.2006.08.014

Prescott, C.E., Zabek, L.M., Staley, C.L., Kabzems, R., 2000. Decomposition of broadleaf and needle litter in forests of British Columbia: influences of litter type, forest type, and litter mixtures. Can. J. For. Res. 30, 1742–1750. https://doi.org/10.1139/x00-097

Probst A., Hernandez L., Fevrier-Vauleon C., Prudent P., Probst J., Party J., 2003. Eléments traces métalliques dans les sols des écosystèmes forestiers français: distribution et facteurs de contrôle -utilisation du réseau RENECOFOR. Office National des Forêts, Direction Technique.

Quantin, P., 2004. Volcanic soils of France. CATENA, Volcanic Soil Resources: Occurrence, Development and Properties 56, 95–109. https://doi.org/10.1016/j.catena.2003.10.019

Rayman, M.P., 2000. The importance of selenium to human health. Lancet 356, 233–241. https://doi.org/10.1016/S0140-6736(00)02490-9

Redon, P.-O., Abdelouas, A., Bastviken, D., Cecchini, S., Nicolas, M., Thiry, Y., 2011. Chloride and organic chlorine in forest soils: storage, residence times, and influence of ecological conditions. Environ. Sci. Technol. 45, 7202–7208. https://doi.org/10.1021/es2011918

Reimann, C., Englmaier, P., Fabian, K., Gough, L., Lamothe, P., Smith, D., 2015. Biogeochemical plant–soil interaction: Variable element composition in leaves of four

559 plant species collected along a south–north transect at the southern tip of Norway. Sci.
560 Total Environ. 506–507, 480–495. https://doi.org/10.1016/j.scitotenv.2014.10.079
561 Ross, H.B., 1985. An atmospheric selenium budget for the region 30° N to 90° N. Tellus B
562 37, 78–90. https://doi.org/10.3402/tellusb.v37i2.14999
563 Roulier, M., Bueno, M., Coppin, F., Nicolas, M., Thiry, Y., Rigal, F., Le Hécho, I., Pannier,
564 F., 2020. Atmospheric iodine, selenium and caesium depositions in France: I. Spatial
565 and seasonal variations. Chemosphere 128971.
566 https://doi.org/10.1016/j.chemosphere.2020.128971
567 Roulier, M., Coppin, F., Bueno, M., Nicolas, M., Thiry, Y., Della Vedova, C., Février, L.,
568 Pannier, F., Le Hécho, I., 2019. Iodine budget in forest soils: Influence of
569 environmental conditions and soil physicochemical properties. Chemosphere 224, 20–
570 28. https://doi.org/10.1016/j.chemosphere.2019.02.060
571 Saeki, K., Matsumoto, S., 1994. Selenite adsorption by a variety of oxides. Commun. Soil
572 Sci. Plant Anal. 25, 2147–2158. https://doi.org/10.1080/00103629409369178
573 Sharma, V.K., McDonald, T.J., Sohn, M., Anquandah, G.A.K., Pettine, M., Zboril, R., 2015.
574 Biogeochemistry of selenium. A review. Environ. Chem. Lett. 13, 49–58.
575 https://doi.org/10.1007/s10311-014-0487-x
576 Söderlund, M., Virkanen, J., Holgersson, S., Lehto, J., 2016. Sorption and speciation of
577 selenium in boreal forest soil. J. Environ. Radioact. 164, 220–231.
578 https://doi.org/10.1016/j.jenvrad.2016.08.006
579 Suess, E., Aemisegger, F., Sonke, J.E., Sprenger, M., Wernli, H., Winkel, L.H.E., 2019.
580 Marine versus Continental Sources of Iodine and Selenium in Rainfall at Two
581 European High-Altitude Locations. Environ. Sci. Technol. 53, 1905–1917.
582 https://doi.org/10.1021/acs.est.8b05533
583 Sun, G.-X., Meharg, A.A., Li, G., Chen, Z., Yang, L., Chen, S.-C., Zhu, Y.-G., 2016.
584 Distribution of soil selenium in China is potentially controlled by deposition and
585 volatilization? Scientific Reports 6. https://doi.org/10.1038/srep20953
586 Supriatin, S., Weng, L., Comans, R.N.J., 2015. Selenium speciation and extractability in
587 Dutch agricultural soils. Sci. Total Environ. 532, 368–382.
588 https://doi.org/10.1016/j.scitotenv.2015.06.005
589 Taylor, S.R., McLennan, S.M., 1995. The geochemical evolution of the continental crust.
590 Rev. of Geophys. 33, 241–265. https://doi.org/10.1029/95RG00262
591 Tolu, J., 2012. Spéciation et mobilité du sélénium présent dans les sols à l'état de traces :
592 contribution aux prévisions à long terme (thesis). Pau.
593 Tolu, J., Le Hécho, I., Bueno, M., Thiry, Y., Potin-Gautier, M., 2011. Selenium speciation
594 analysis at trace level in soils. Anal. Chim. Acta 684, 126–133.
595 https://doi.org/10.1016/j.aca.2010.10.044
596 Tolu, J., Thiry, Y., Bueno, M., Jolivet, C., Potin-Gautier, M., Le Hécho, I., 2014. Distribution
597 and speciation of ambient selenium in contrasted soils, from mineral to organic rich.
598 Sci. Total Environ. 479–480, 93–101. https://doi.org/10.1016/j.scitotenv.2014.01.079
599 Tyler, G., 2005. Changes in the concentrations of major, minor and rare-earth elements
600 during leaf senescence and decomposition in a Fagus sylvatica forest. For. Ecol.
601 Manag. 206, 167–177. https://doi.org/10.1016/j.foreco.2004.10.065
602 Ulrich, E., Coddeville, P., Lanier, M., 2002. Retombées atmosphériques humides en France
603 entre 1993 et 1998. ADEME, Paris.
604 Wang, S., Liang, D., Wang, D., Wei, W., Fu, D., Lin, Z., 2012. Selenium fractionation and
605 speciation in agriculture soils and accumulation in corn (Zea mays L.) under field
606 conditions in Shaanxi Province, China. Sci. Total Environ. 427–428, 159–164.
607 https://doi.org/10.1016/j.scitotenv.2012.03.091

608 Wen, H., Carignan, J., 2007. Reviews on atmospheric selenium: Emissions, speciation and
609 fate. Atmos. Environ. 41, 7151–7165. https://doi.org/10.1016/j.atmosenv.2007.07.035
610 Weng, L., Vega, F.A., Supriatin, S., Bussink, W., Riemsdijk, W.H.V., 2011. Speciation of Se
611 and DOC in Soil Solution and Their Relation to Se Bioavailability. Environ. Sci.
612 Technol. 45, 262–267. https://doi.org/10.1021/es1016119
613 Wessjohann, L.A., Schneider, A., Abbas, M., Brandt, W., 2007. Selenium in chemistry and
614 biochemistry in comparison to sulfur. Biol. Chem. 388, 997–1006.
615 https://doi.org/10.1515/BC.2007.138
616 Winkel, L.H.E., Vriens, B., Jones, G.D., Schneider, L.S., Pilon-Smits, E., Bañuelos, G.S.,
617 2015. Selenium cycling across soil-plant-atmosphere interfaces: A critical review.
618 Nutrients 7, 4199–4239. https://doi.org/10.3390/nu7064199
619

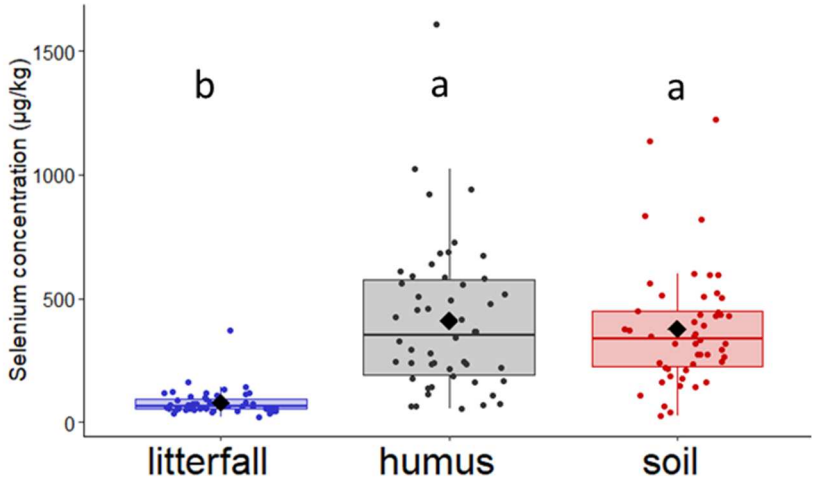

Figure 1. Selenium concentrations in litterfall, humus and soils. Box plots show the first quartile (Q_1), median and third quartile (Q_3) of the data. Black diamond symbols represent average Se concentrations in groups. Lower and upper whiskers extend from the hinges by Q_1 - 1.5 × IQR (IQR - interquartile range) and Q_3 + 1.5 × IQR, respectively. Dots represent corresponding data. The different letters above the boxes correspond to significant differences between the groups according to pairwise Wilcoxon test, with Holm adjustment for p-value.

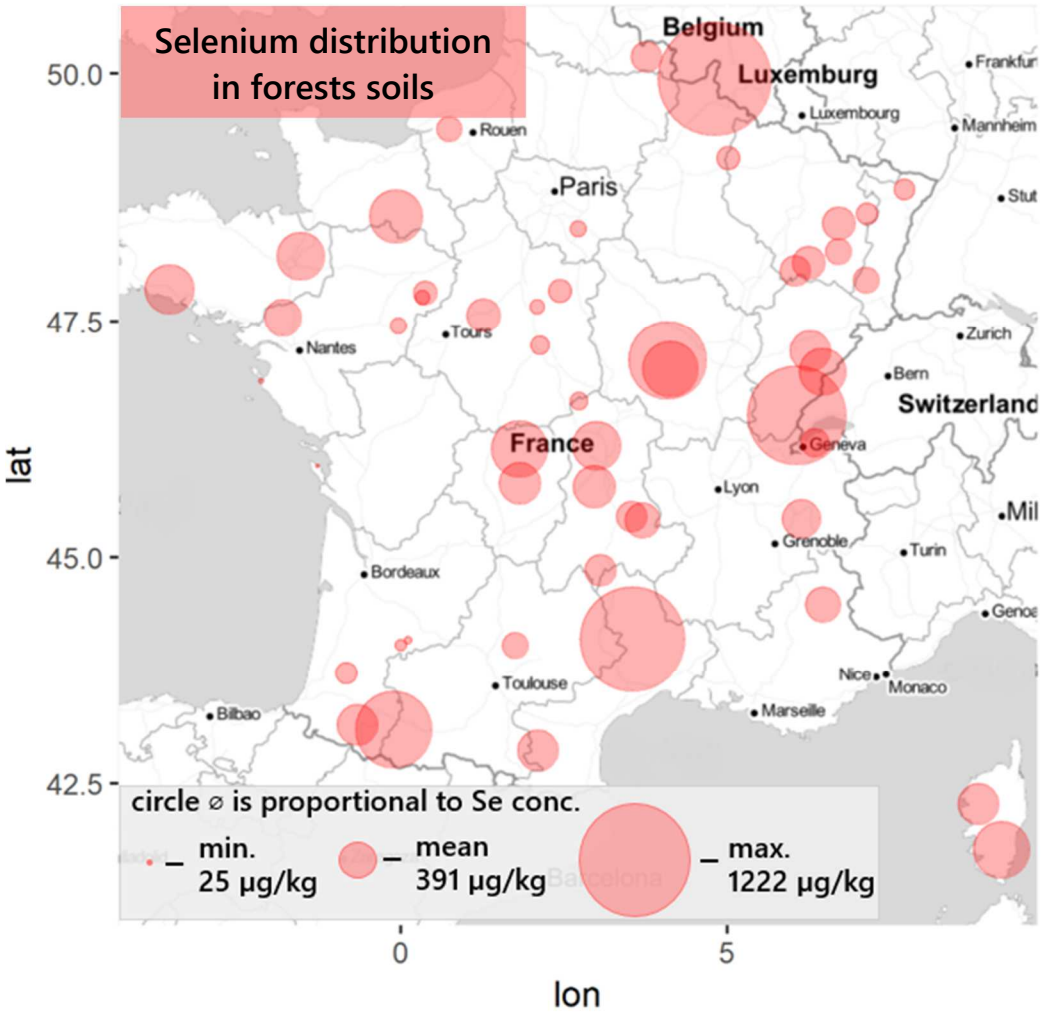

Figure 2 Selenium concentrations in French forest soils (mean value of top 40 cm soil). Diameter of red circle is proportional to Se concentration (minimun: 25 µg kg^{-1}; maximum: 1222 µg kg^{-1}).

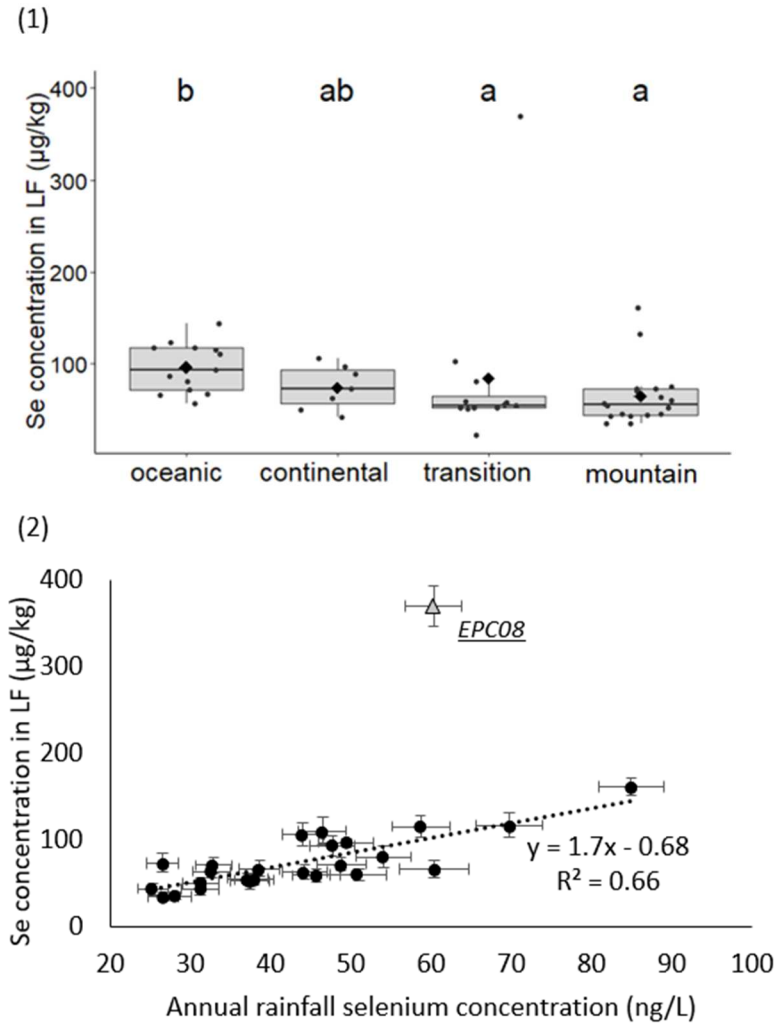

Figure 3 Se concentration in litterfall according to 1) climate; 2) annual volume-weighted mean Se concentration in rainfall. In Figure 3.1 box plots show the first quartile (Q_1), median and third quartile (Q_3) of the data. Black diamond symbols represent average Se concentrations in groups. Lower and upper whiskers extend from the hinges by Q_1 - 1.5 × IQR (IQR - interquartile range) and Q_3 + 1.5 × IQR, respectively. Dots represent corresponding data. The different letters above the boxes correspond to significant differences between the groups according to pairwise Wilcoxon test, with Holm adjustment for p-value.

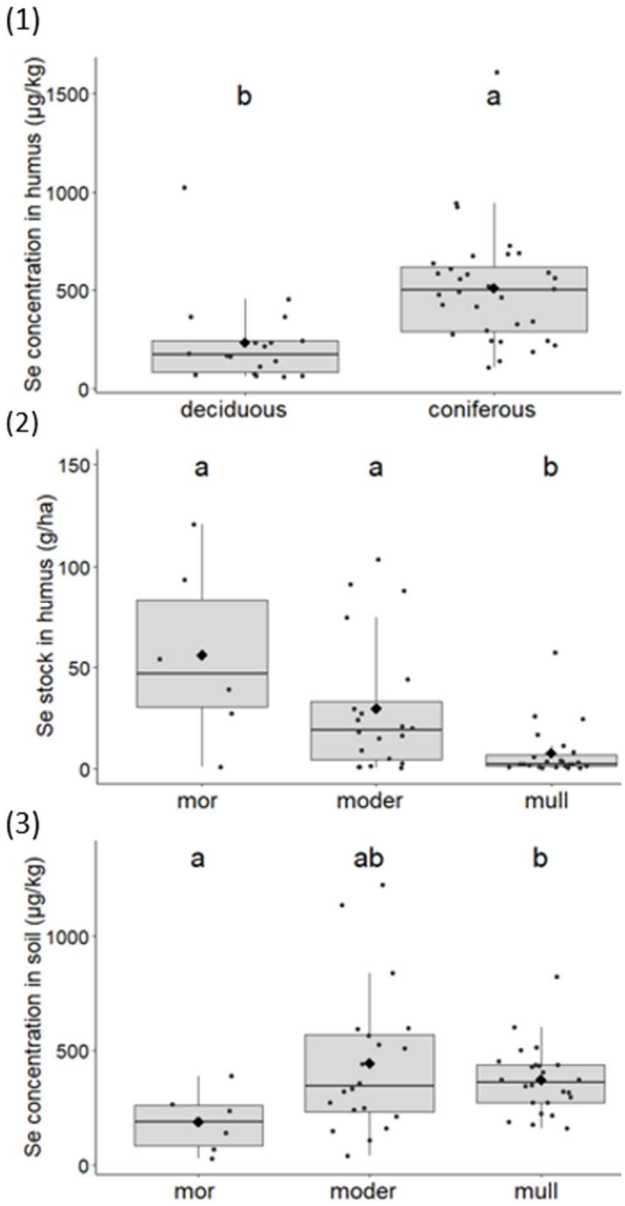

Figure 4 Boxplot representations of: 1) Se concentrations in humus according to forest type; 2) Se stocks in humus according to humus type; 3) Se concentrations in soils according to humus type. Box plots show the first quartile (Q_1), median and third quartile (Q_3) of the data. Black diamond symbols represent average Se concentrations in groups. Lower and upper whiskers extend from the hinges by Q_1 - 1.5 × IQR (IQR - interquartile range) and Q_3 + 1.5 × IQR, respectively. Dots represent corresponding data. The different letters above the boxes correspond to significant differences between the groups according to pairwise Wilcoxon test, with Holm adjustment for p-value.

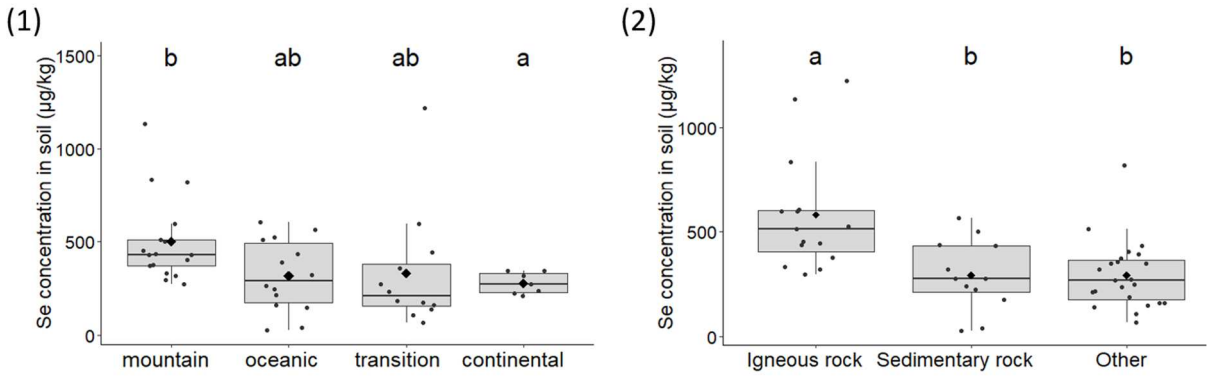

Figure 5 Distribution of Se concentrations in soils according to 1) climate, and 2) rock type. Box plots show the first quartile (Q_1), median and third quartile (Q_3) of the data. Black diamond symbols represent average Se concentrations in groups. Lower and upper whiskers extend from the hinges by $Q_1 - 1.5 \times IQR$ (IQR - interquartile range) and $Q_3 + 1.5 \times IQR$, respectively. Dots represent corresponding data. The different letters above the boxes correspond to significant differences between the groups according to pairwise Wilcoxon test, with Holm adjustment for p-value.

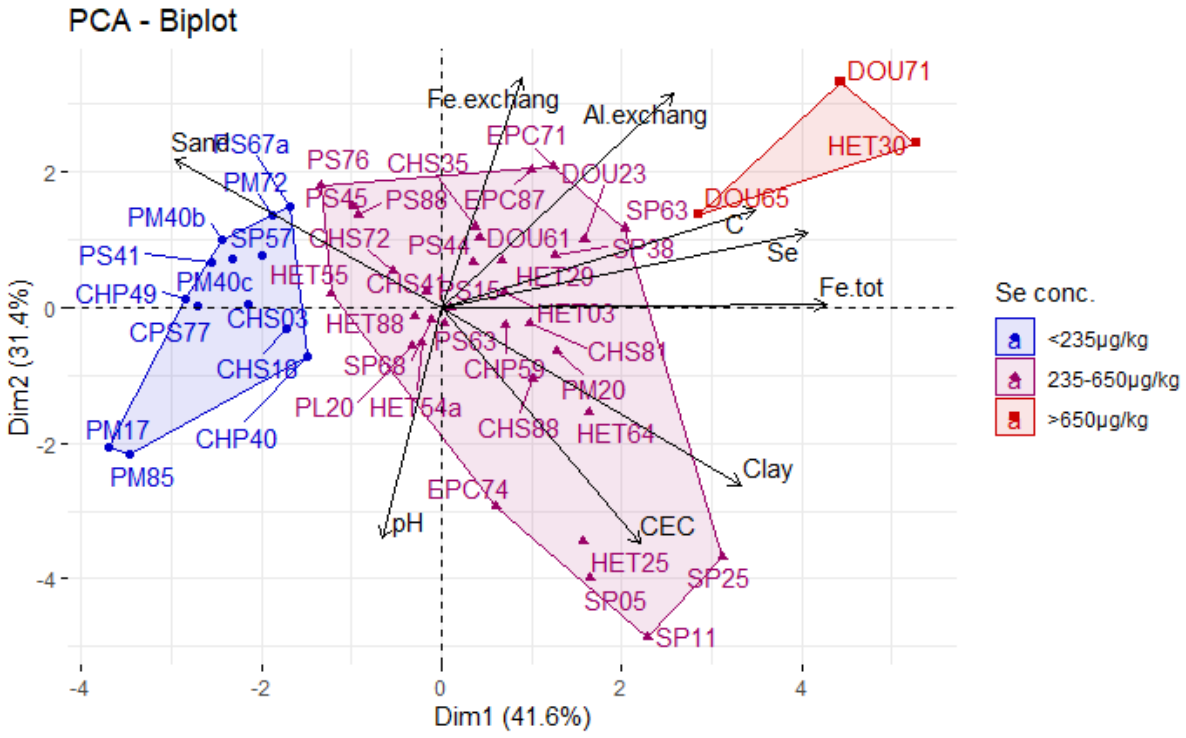

Figure 6 PCA biplot representation of soil composition data on the first two PC axis . Individual soils (48 samples) are colored according to their Se concentration range: : <235 µg kg^{-1} - blue, 235-650 µg kg^{-1} - violet, >650 µg kg^{-1} - red. Arrows represent contribution of soil geochemical numerical variables on principal component axes.

Table 1 Statistical analysis for Se concentrations in soil, humus and litterfall. Spearman rank correlation coefficient r_s and Kruskal-Wallis χ^2 values with p-values. Significant correlations are marked in bold.

	Variables	soil		humus		litterfall	
Numerical variables		r_s	p	r_s	p	r_s	p
	Coastal distance	-0.02	0.880	-0.02	0.885	**-0.35**	**< 0.05**
	Se conc. in rain[1]	-0.13	0.530	0.23	0.267	**0.76**	**< 0.001**
	Se flux in rain[1]	0.34	0.087	0.31	0.123	**0.41**	**< 0.05**
	Se flux in litterfall and rain	0.13	0.530	0.21	0.309		
	Se accumulation rate in humus	**0.43**	**< 0.01**				
Categorical variable		χ^2	p	χ^2	p	χ^2	p
	Tree species (n=6)	**22.58**	**< 0.001**	**20.25**	**< 0.01**	7.24	0.203
	Forest type (n=2)	0.17	0.682	**15.53**	**< 0.001**	0.15	0.697
	Climate (n=4)	**10.74**	**< 0.05**	3.97	0.265	**11.36**	**< 0.01**
	Humus type (n=3)	**6.02**	**< 0.05**	5.26	0.072		
	Rock type (n=3)	**16.34**	**< 0.001**				
	Soil type (n=7)	12.61	0.082				

[1] test performed for 27 sites; n - number of sub-types

Table 2 Contributions on the first three PC axes of i) all variables and ii) reduced number of variables.

Variables	i) contributions of all variables			ii) contribution of reduced number of variables		
	Dim.1	Dim.2	Dim.3	Dim.1	Dim.2	Dim.3
Fe tot	15.806	5.64E-05	0.067	21.585	5.498	0.610
Se	14.990	1.683	0.003	23.708	1.522	1.481
N	13.898	0.744	6.801	-	-	-
Al tot	12.761	3.301	3.463	-	-	-
C_{org}	12.262	5.510	5.761	19.620	0.378	17.124
Clay	8.555	11.535	0.071	-	-	-
Sand	6.962	12.615	9.032	3.853	17.197	50.116
Al exchang.	5.627	10.315	10.237	18.698	5.902	3.600
Silt	3.946	9.073	17.462	-	-	-
CEC	3.637	14.145	8.354	0.282	34.693	0.471
Mn exchang.	0.859	5.798	10.039	-	-	-
pH	0.364	9.701	26.421	5.268	20.562	23.163
Fe exchang.	0.333	15.580	2.288	6.987	14.248	3.435

exchang. – exchangeable